Structure of the Fivefold Surface of the Icosahedral Al-Cu-Fe Quasicrystal: Experimental Evidence of Bulk Truncations at Larger Interlayer Spacings

H. R. Sharma,[1,*] V. Fournée,[2] M. Shimoda,[1,3] A. R. Ross,[4] T. A. Lograsso,[4] A. P. Tsai,[1,3,5] and A. Yamamoto[6]

[1]*SORST, Japan Science and Technology Agency, Japan*

[2]*LSG2M, CNRS-UMR7584, Ecole des Mines, Parc de Saurupt, 54042 Nancy, France*

[3]*National Institute for Materials Science, 1-2-1 Sengen, Tsukuba, Ibaraki, 305-0047, Japan*

[4]*Department of Materials Science and Engineering, Ames Laboratory, Ames, Iowa 50011, USA*

[5]*Institute of Multidisciplinary Research for Advanced Materials, Tohoku University, Sendai, 980-8577, Japan*

[6]*Advanced Materials Laboratory, National Institute for Materials Science, Tsukuba, Ibaraki, 305-0044, Japan*

(Received 5 July 2004; published 14 October 2004)

Based on scanning tunneling microscopy of the fivefold surface of the icosahedral Al-Cu-Fe quasicrystal and the refined structure model of the isostructural *i*-Al-Pd-Mn, we present evidence that the surface corresponds to bulk truncations at the positions where blocks of atomic layers are separated by larger interlayer spacings (gaps). Both step-height distribution and high resolution scanning tunneling microscopy images on terraces reveal bulk truncations at larger gaps.

DOI: 10.1103/PhysRevLett.93.165502 PACS numbers: 61.44.Br, 68.35.Bs, 68.37.Ef

Quasicrystals are solids with aperiodic long-range order frequently associated with rotational symmetries forbidden to ordinary crystals. Among the widely investigated stable quasicrystals are the face-centered icosahedral (*i*) phases of the *i*-Al-Pd-Mn family that includes *i*-Al-Cu-Fe [1]. Their bulk structure is usually described by an ideal model, which is characterized by an infinite number of rigorously nonidentical flat atomic layers stacked quasiperiodically along any direction [2]. Despite their complex aperiodic structure, quasicrystals under suitable preparation conditions yield atomically flat terraced surfaces characteristic of bulk truncations [3–9]. However, a theoretical explanation of the stability of such a terraced structure is still lacking.

The stability of ordinary crystal surfaces is widely described by a well-known empirical rule stating that crystal surfaces correspond to the bulk planes with maximum atomic density [10]. The direct application of this conventional rule to icosahedral quasicrystals is, however, impossible because these have no planes with the same density in general. Recently, a modified density rule has been proposed to explain the surface termination of icosahedral quasicrystals [11]. This rule considers the density of nearby dense planes, instead of a single plane and suggests that the surface terminates at planes with relatively larger density. This modified rule, however, was found to be inadequate to describe every observed feature. Especially, it cannot explain why only one of two equivalent pairs of planes with identical maximum density but with different orientations appears at the surface [11].

In this Letter, we present a structural analysis of the fivefold *i*-Al-Cu-Fe surface based on new scanning tunneling microscopy (STM) results and a recent refined structure model of the isostructural *i*-Al-Pd-Mn [1,12], instead of the ideal (unrelaxed) models. We find that the surface corresponds to the bulk truncations at the positions where blocks of atomic layers are separated by larger interlayer spacings (gaps). This simple rule that the bulk terminates at larger gaps can be easily understood in ionic crystals from the physico-chemical point of view, since it is conceivable that the strength of chemical bonds decreases rapidly with the increase of interatomic distances larger than an optimum value. For metals such as quasicrystals, however, this is not clear enough since the electronic wave function spreads over the entire crystal volume and the stability of surfaces may be closely related with the electronic band structure. Our findings thus open an intriguing problem to be solved theoretically on the appearance and/or stability of quasicrystal surfaces.

For the surface preparation, a single grain $Al_{63}Cu_{24}Fe_{13}$ sample was cut along the fivefold plane and mechanically polished using diamond paste down to 0.25 μm. Subsequently, repeated cycles of Ar^+ sputtering (1-3 keV, 30 minutes) and annealing (up to about 750 °C, 15-20 minutes) were carried out in the ultrahigh vacuum chamber (base pressure 1×10^{-10} mbar) until no oxygen was detectable by x-ray photoemission spectroscopy. Temperature was measured using an optical pyrometer (emissivity, $\epsilon = 0.35$). The employed annealing temperature is about 150 °C higher than that of previous studies on the same surface [3,6,7]. For our sample, such a higher annealing temperature was needed to yield a step-terrace structure. The chemical composition of the thus prepared surface determined by measuring the intensity of Al 2s, Cu 2*p*, and Fe 2*p* core level photoemission is found to be close to the bulk composition and therefore possible evaporation of the constituent elements during surface preparation can be ruled out. STM images were recorded at room temperature with an Omicron STM with tunneling currents of 0.15-0.25 nA and bias voltages of 1.0-2.6 V.

Scanning tunneling microscopy of the surface reveals fairly large terraces (up to μm scale along the step edge) separated by steps of different heights [Fig. 1(a)–1(d)]. The observed step heights are presented in Table I. For the step-height determination, we sample 300 steps from images (over about 40 μm^2 scanned area) recorded on different parts of the surface obtained in different cleaning cycles. Then the height of each individual step is calculated by the distribution of measured z values in the immediate vicinity of the step. These individual step heights are used to calculate the average value of the respective step heights. (In our analysis, steps with distances smaller than a few nm are treated as a single step of combined height.) All observed step heights (h) can be obtained by linear combination of 0.37 nm ($=L$, long) and L/τ ($=S$, short), i.e., $h \approx mS + nL$, with (m,n) integers and $\tau = 1.618\ldots$, the golden mean.

Among sample of 300 steps, the steps of 0.58 nm ($S + L$) and 0.96 nm ($S + 2L$) height are observed most frequently. The occurrence of the 0.37 nm (L), 1.55 nm ($2S + 3L$) and 2.52 nm ($3S + 5L$) high steps is also fairly frequent. The number of (S, L) steps (given by (m,n) values in Table I) that build these frequently observed steps are (0,1), (1,1), (1,2), (2,3), and (3,5), which constitute the sets of six successive Fibonacci numbers. (Fibonacci numbers are 0, 1, 1, 2, 3, 5, 8, 13, ..., where each number is the sum of the two previous ones). This implies that the steps prefer to be formed with Fibonacci numbers of S and L steps. Figure 1(c) shows such an example, where numbers of S and L steps present in marked steps represent five successive Fibonacci numbers. The other steps of S, $2S + 2L$ and $S + 3L$ height run in an extremely narrow region of the terraces, wandering, and often appear as a bridge between these frequently observed bunched steps which generally run in a fairly large distance (up to several hundreds nm) and tend to orient along a specific direction. These features as well as their low occurrence indicate that the surface termination with S, $2S + 2L$ and $S + 3L$ steps is less preferable.

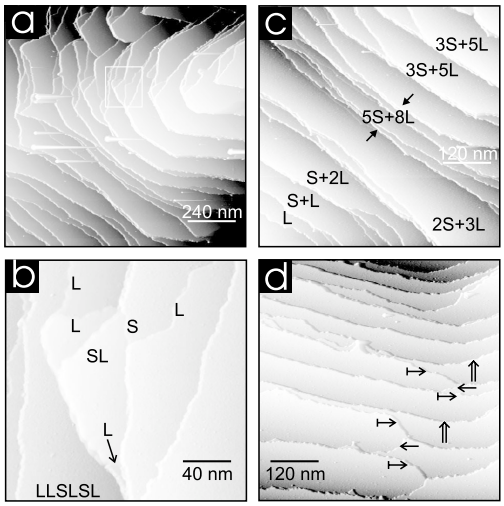

FIG. 1. STM images of the fivefold i-Al-Cu-Fe surface (a)–(d): (b) the area marked by white frame in image (a) in a magnified scale showing individual L and S steps, (c) steps formed with Fibonacci numbers of S and L steps, and (d) sequence of $L(\rightarrow)$, $S + L(\mapsto)$ and $S + 2L(\Rightarrow)$ steps.

Since the majority of observed steps are perfectly bunched, it is not always possible to identify the sequence of L and S steps. However, in a few parts of images, we were able to identify single steps which appear as a section of a Fibonacci sequence. For example, the observed $LLSLSL$ sequence in Fig. 1(b) is a part of a Fibonacci sequence, $LSLLSLSL\ldots$ (A Fibonacci sequence can be generated by taking a segment, L and applying an inflation rule, $L \rightarrow LS$ and $S \rightarrow L$). Occasionally, in different parts of the surface, steps of $S + L$ and L or $S + 2L$ and $S + L$ or $2S + 3L$ and $S + 2L$ height (not shown) appear in a Fibonacci sequence, which may represent a section of a sequence obtained by deflating original Fibonacci sequence, $LSLLSLSL\ldots$. With these observed Fibonacci sequences as well as the fact that step heights corresponding to segments forbidden for a Fibonacci sequence, such as LLL and $LSLSLS$, were not observed (Table I), we conclude that the stacking of L and S steps follows a Fibonacci sequence.

Almost all observed features of the step-height distribution can be strictly explained in terms of a structure model of i-Al-Pd-Mn obtained after refinement of an ideal bulk structure by using x-ray diffraction data [1,12]. The R factor after crystallographic refinement is comparable to those achieved for usual crystals. The refinement results in shifts of most atoms from their ideal positions of the order of 0.03 nm. Consequently, most of small gaps existing in the ideal structure disappear. The remaining gaps normal to the fivefold axis can be categorized into three types according to their size: *large gaps* of size 0.115 ($\pm$0.010) nm, *medium gaps* of size 0.07 ($\pm$ 0.01) nm, and remaining *small gaps* of smaller size. The separation between consecutive *large* or *medium gaps* (without considering *small gaps*) takes one of the

TABLE I. Observed step-heights, $h \approx mS + nL$, with $L =$ 0.37 nm and $S = L/\tau$ and their occurrence (σ: standard deviation).

Step-height/nm	(m,n)	$mS + nL$	Occurrence
0.21 ($\sigma = 0.02$)	(1,0)	S	3%
0.37 ($\sigma = 0.02$)	(0,1)	L	14%
0.58 ($\sigma = 0.02$)	(1,1)	$S + L$	32%
0.96 ($\sigma = 0.03$)	(1,2)	$S + 2L$	29%
1.20 ($\sigma = 0.01$)	(2,2)	$2S + 2L$	1%
1.37 ($\sigma = 0.02$)	(1,3)	$S + 3L$	1%
1.55 ($\sigma = 0.03$)	(2,3)	$2S + 3L$	15%
1.95 ($\sigma = 0.03$)	(2,4)	$2S + 4L$	1%
2.52 ($\sigma = 0.04$)	(3,5)	$3S + 5L$	4%

two values, 0.24 ($\pm$0.04) nm and 0.40 ($\pm$0.03) nm, and follows a Fibonacci sequence. The refined structure hence can be viewed as thick and thin blocks of atoms stacked in a Fibonacci sequence along the fivefold axis with *medium* or *large gaps* between them as shown in Fig. 2(a).

The observed Fibonacci sequence of L and S steps is found to be consistent with the stacking of the thick and thin blocks, indicating that the surface forms at the position of *large* and *medium gaps*. However, as described earlier, STM data suggest that the formation of S steps is less favorable in comparison with L, $S + L$, and $S + 2L$ steps. This can be understood because preferential surface termination only at *large gaps* would yield L, $S + L$, and $S + 2L$ steps (that does not include S steps) in agreement with observations [see Fig. 2(b)]. Moreover, the sequence of L, $S + L$ and $S + 2L$ steps of this termination can be also identified in STM images (compare sequences shown in Fig. 1(d) and 2(b)]. The occurrence ratio of these steps estimated from a cluster of 20 nm size along the fivefold axis is found to be about 0.5:1:0.3, i.e., with occurrence of $S + 2L$ steps less frequent than observed experimentally (see Table I).

To explain frequent occurrence of the $S + 2L$ steps, the atomic density in the top region of the blocks needs to be considered, in addition to the magnitude of the gaps separating the blocks. For a given thickness of the top region, the atomic density varies in each block. For instance, the density varies from a value comparable to that of a close-packed Al(111) fcc surface down to 30% thereof for the region of the top 0.06 nm. The surface termination at *large gaps* above regions of moderate or high density would produce frequent occurrence of $S + 2L$ steps [Fig. 2(c)] in agreement with the observation.

The origin of the $2S + 3L$, $2S + 4L$, and $3S + 5L$ steps can be explained by surface termination at *large gaps* above regions of high density [Fig. 2(d)]. An alternative explanation for the appearance of these higher steps is provided by considering the chemical composition of the block. Like the density, the composition also varies in each block. The relative Al concentration in the region of the top 0.06 nm can vary from 70% to 99%. We note that Al has a lower surface free energy than the other elements. Previous studies based on dynamical low-energy electron diffraction [6,13] and x-ray photoelectron diffraction [14] have shown that the fivefold *i*-Al-Pd-Mn and *i*-Al-Cu-Fe surfaces form at dense Al-rich planes. Considering surface termination at blocks with Al concentration >97% can equally produce these higher steps (not shown). Interestingly, these ideal terminations (on high density blocks or on Al-rich blocks) do not yield $2S + 2L$ and $S + 3L$ steps, in agreement with the observation that these steps almost never appear in the STM images. In summary, the characteristics of the observed step-height distribution can be explained in every detail by the refined model assuming simple rules that the surface terminates preferentially at *large gaps* above regions of relatively large atomic density and high Al content. Here, we recall previous observations that the most stable surfaces in *i*-Al-Pd-Mn are normal to the

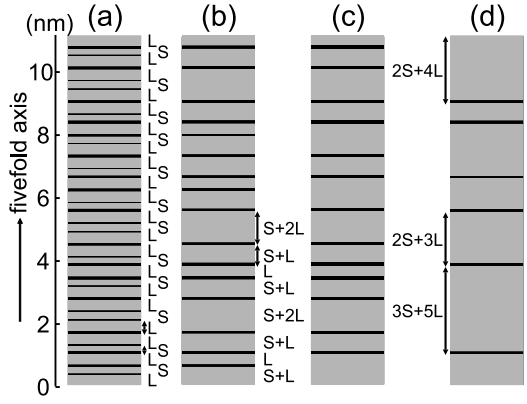

FIG. 2. Schematic view of the refined structure of *i*-Al-Pd-Mn projected normal to the fivefold axis (gray and black rectangles depict blocks of layers and gaps, respectively) showing (a) *medium* and *large gaps*, (b) only *large gaps*, (c) *large gaps* above regions of a moderate or high density, and (d) *large gaps* above regions of a high density.

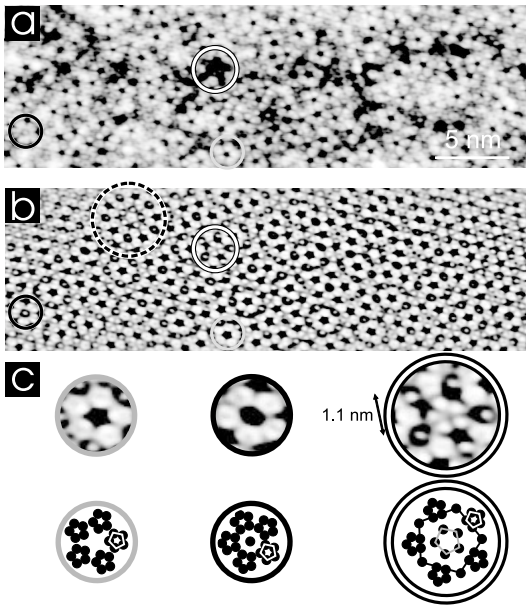

FIG. 3. (a) High resolution STM image of the fivefold *i*-Al-Cu-Fe surface displaying three different repeating motives represented by circles of different colors. (b) Fourier transform pass filtering of image (a). (c) Motives from the filtered image in magnified scale and their description in terms of atomic position. For smallest pentagons (white) appearing in different parts, the occupation probability of the vertices is unity or nonunity. The edge length of the marked pentagons is related by $\sim 1{:}\tau{:}\tau^3$. A slight distortion of the motives from a perfect pentagonal symmetry may be attributed to thermal drift during scanning and/or limits in the piezo calibration.

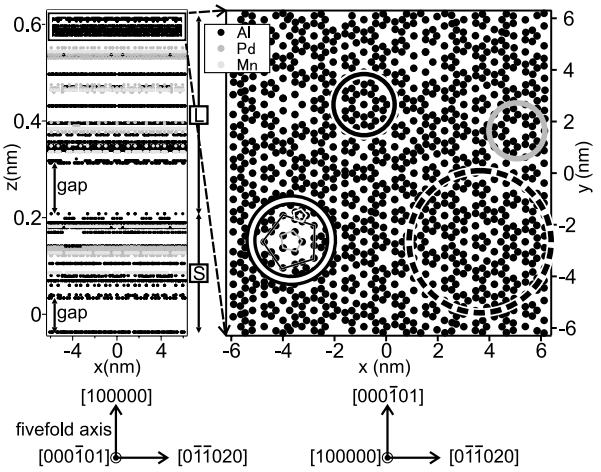

FIG. 4. Left: a section of the refined structure of *i*-Al-Pd-Mn projected normal to the fivefold axis showing a thick and a thin block of layers. The horizontal axis is compressed to highlight gaps. Right: in-plane structure in the region of the top 0.04 nm of a thick block (marked by a rectangle). The composition is pure Al and the atomic density matches the density derived from STM images ($\sim$8 atoms/nm^2). Circles (and pentagons) of different colors mark the identical features (and pentagons) observed in STM images (Fig. 3). Indexing follows Ref. [1].

fivefold axis [15]. Since the refined structure possesses largest gaps normal to the fivefold axis than those for other directions, the higher stability of the fivefold surface thus can be understood again by the preferential surface terminations at larger gaps.

Further evidence of the surface termination at larger gaps is revealed by comparing high resolution STM images with the in-plane structure of the model. STM image shown in Fig. 3(a) predominantly exhibits three different motives, representative of which are marked by circles of different colors. To highlight these motives, we calculate Fourier transform pass filtering taking all observable maxima in the Fourier transform of the image [Fig. 3(b)]. The given STM image was recorded from a terrace with *L* step. It is thus reasonable to compare this image with the atomic structure in the top region of a thick block. The in-plane structure indeed exhibits features (marked by circles of different colors, Fig. 4) undoubtedly identical to the STM motives in every detail such as length scale, orientation, occupation probability of the vertices of the smallest pentagons, and local arrangement (see, for example, alternate appearance of two motives forming a ring, marked by a dotted circle). We thus conclude that a good agreement exists between the bulk truncations at larger gaps and our STM images, for the in-plane structure as well as along the surface normal. It further suggests that the fivefold surfaces of *i*-Al-Pd-Mn and *i*-Al-Cu-Fe are isostructural, and that differences reported earlier [7] were mainly due to tip effects.

Finally, we note that in contrast to the present observations, the surface prepared at lower annealing temperature shows *L*- and *S* + *L*-step configurations [4–9], screw dislocations, and high density of shallow pentagonal pits.

To summarize, we presented an analysis of STM results on the fivefold *i*-Al-Cu-Fe surface based on a refined bulk structure model of the isostructural *i*-Al-Pd-Mn. Both step-height distribution and high resolution images on terraces strongly reveal that the surface corresponds to the bulk truncations at larger interlayers spacings. For metals such as quasicrystals possessing electronic wave functions spreading over the entire crystal volume, the surface termination at larger interlayer spacings is yet to be explained theoretically.

This work was partially supported by SORST, JST and GASR, Ministry of ECSST, Japan. We thank W. Theis and F. U. Berlin for critical reading of the manuscript.

*Corresponding author.
Electronic address: hemraj.sharma@nims.go.jp

[1] A. Yamamoto, H. Takakura, and A. P. Tsai, Phys. Rev. B **68**, 094201 (2003).
[2] M. Boudard, M. de Boissieu, C. Janot, G. Heger, C. Beeli, H.-U. Nissen, H. Vincent, R. Ibberson, M. Audier, and J. M. Dubois, J. Phys. Condens. Matter **4**, 10 149 (1992).
[3] R. S. Becker, A. R. Kortan, F. A. Thiel, and H. S. Chen, J. Vac. Sci. Technol. B **9**, 867 (1991).
[4] T. M. Schaub, D. E. Bürgler, H.-J. Güntherodt, and J. B. Suck, Phys. Rev. Lett. **73**, 1255 (1994).
[5] Z. Shen, C. R. Stoldt, C. J. Jenks, T. A. Lograsso, and P. A. Thiel, Phys. Rev. B **60**, 14 688 (1999).
[6] T. Cai *et al.*, Surf. Sci. **495**, 19 (2001).
[7] T. Cai, V. Fournée, T. Lograsso, A. Ross, and P. A. Thiel, Phys. Rev. B **65**, 140202 (2002).
[8] Z. Papadopolos, G. Kasner, J. Ledieu, E. J. Cox, N. V. Richardson, Q. Chen, R. D. Diehl, T. A. Lograsso, A. R. Ross, and R. McGrath, Phys. Rev. B **66**, 184207 (2002).
[9] L. Barbier, D. L. Floc'h, Y. Calvayrac, and D. Gratias, Phys. Rev. Lett. **88**, 085506 (2002).
[10] J. D. H. Donnay and D. Harker, Am. Mineral. **22**, 446 (1937).
[11] Z. Papadopolos, P. Pleasants, G. Kasner, V. Fournée, C. J. Jenks, J. Ledieu, and R. McGrath, Phys. Rev. B **69**, 224201 (2004).
[12] A. Yamamoto, H. Takakura, and A. P. Tsai, J. Alloys Compd. **342**, 159 (2002).
[13] M. Gierer, M. A. V. Hove, A. I. Goldman, Z. Shen, S.-L. Chang, C. J. Jenks, C.-M. Zhang, and P. A. Thiel, Phys. Rev. Lett. **78**, 467 (1997).
[14] J.-C. Zheng *et al.*, Phys. Rev. B **69**, 134107 (2004).
[15] Z. Shen *et al.*, Surf. Sci. **450**, 1 (2000).